AIAA JOURNAL
Vol. 45, No. 6, June 2007

Controlling Volumetric Heat Release Rates in a Dump Combustor Using Countercurrent Shear

A. A. Behrens* and P. J. Strykowski†
University of Minnesota, Minneapolis, Minnesota 55455

DOI: 10.2514/1.24059

Research carried out in a backward-facing step combustor burning prevaporized JP10–air mixtures has examined the implementation of counterflow as a means to enhance turbulent combustion and increase volumetric heat release rates. The combustor is characterized by a nominally two-dimensional primary flow of lean reactants entering a rectangular channel before encountering a 2:1 single-sided step expansion. A secondary flow is created via suction at the dump plane as a fluidic control mechanism to enhance the naturally occurring countercurrent shear layer caused by separation. Counterflow is shown to elevate turbulence levels and volumetric heat release rates downstream of the step while concomitantly reducing the scale of the recirculation zone. Modifications to the rearward-facing step geometry are investigated using particle image velocimetry under isothermal flow conditions in an effort to extend the near-field interaction between the recirculation zone and the incoming primary flow, further exploiting the benefits of counterflow. Relative heat release rates quantified using chemiluminescence are shown to increase by 70% with a counterflow level of 6% of the primary mass flow rate in the step geometry, and by 150% when 3.5% counterflow is introduced into a modified step geometry.

Introduction

REARWARD-FACING step geometries have been studied extensively in an effort to create compact, low-drag combustors with wide turndown for high-speed propulsion applications such as ramjet and scramjet engines. Dump combustors provide an attractive geometry as the flow separation over the sudden expansion provides an energetic mechanism for turbulence production and the low-speed zone behind the step is conducive for flame anchoring [1,2]. Research has focused on understanding the basic flowfield under isothermal and reacting conditions, with particular interest in the drag characteristics of the separated flow and reattachment point [2–6], instabilities associated with confined combustion [7–9], and methods for enhancing global heat release rates [10]. Results presented in this paper focus on fluidic control of the flowfield using a countercurrent shear layer, with the overall objective of increasing volumetric heat release rates in the zone downstream of the step.

Countercurrent shear has been studied in confined and unconfined geometries over the past decade, and has been shown to increase turbulence production, turbulence length scales, and flow three-dimensionality, as compared with coflowing layers having comparable shear [11–14]. Furthermore, dramatic mixing enhancement has been observed for both incompressible and compressible mixing layers and jets, indicating the scalability of the approach [12,13]. Previous work conducted in a dump combustor geometry under isothermal flow conditions [11] suggests that this control strategy should be effective at creating compact combustion with elevated burning velocities. These possible benefits are desirable for high-speed combustion applications in which mixing and residence time scales are very short.

The first systematic studies of countercurrent shear were motivated by observations from linear stability theory, which revealed that isothermal shear layers would experience a transition from convective to absolute instability at sufficiently high velocity ratios [15–18]. Experimental studies in axisymmetric jets corroborated the connection between the stability concepts and the global flow response for both isothermal and variable density flows [15,16]. Recent investigations of self-similar turbulent countercurrent shear layers have yielded new insight into the manifestations of the apparent stability transition as it plays out at conditions well removed from the linear limit [14]. Self-similar mean velocity profiles were found to be nominally invariant over a range of velocity ratios ranging from $R = 1.0$–1.85, where $R = (U_1 - U_2)/(U_1 + U_2)$, whereas the turbulent stresses experienced a strong bifurcation at $R \sim 1.3$. This critical velocity ratio was in remarkable agreement with predictions from linear stability analysis [14,17]; turbulent energy production, critical for enhancing turbulent combustion, followed a trend similar to the turbulent stresses. Although many aspects of turbulent countercurrent shear flows are not fully understood, the initial observations did reveal increased isotropy, entrainment, and flow three-dimensionality for velocity ratios above $R \sim 1.3$. Results from recent isothermal studies in the backward-facing step geometry [11] show that countercurrent shear maximizes the production of turbulent energy and increases turbulence length scales for a given level of shear, while keeping filtered strain rates essentially unchanged. These characteristics motivated the implementation of countercurrent shear as a flow control technique for combustion enhancement.

A dump combustor in the form of an asymmetric rearward-facing step was selected as a combustor model for implementation of countercurrent shear. This configuration is relevant to ramjet/scramjet systems but is sufficiently generic to address the more basic question of the control of bluff-body flame holders as seen in gas turbine combustors and afterburners. Figure 1 shows the conventional and countercurrent shear dump combustor. The conventional dump combustor produces a flowfield containing naturally occurring reverse flow caused by separation. This is a geometry that is efficient at producing high turbulence levels while providing a low-speed zone for flame anchoring, though it suffers from severe drag penalties [1,2]. The method used to employ countercurrent shear control was based on a suction approach, implemented by the placement of a vacuum cavity behind the step; momentum driven countercurrent shear was not selected largely due to difficulties handling lean mixtures of JP10–air, i.e., to avoid fuel condensation in the secondary delivery lines. A narrow gap on the downstream-facing step wall near the trailing edge, seen in Fig. 1b, allows for the removal of gas from the combustor, thereby manipulating both the separating shear layer and nature of the

Received 20 March 2006; revision received 19 January 2007; accepted for publication 19 January 2007.

*Graduate Research Assistant, Department of Mechanical Engineering.
†Professor, Department of Mechanical Engineering. Senior Member AIAA.

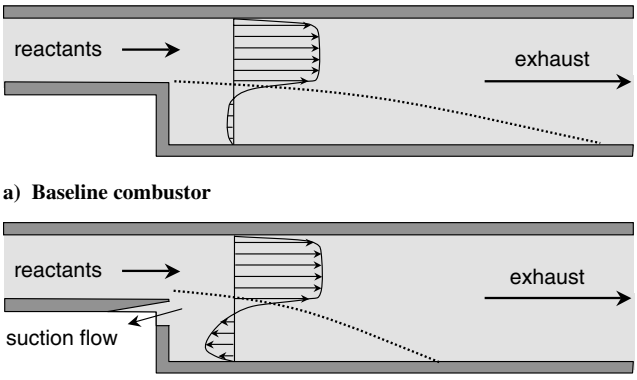

Fig. 1 Shear dump combustor: a) conventional, and b) countercurrent.

recirculation flow downstream of the step. As shown in isothermal studies [11], the gas drawn from the recirculation zone serves to drive a countercurrent shear layer as the flow separates off the step. It also affects the size of the recirculation zone as the lower wall attachment point moves upstream.

Experimental Setup

The experiments were conducted at the Shear Flow Control Laboratory of the University of Minnesota. Figure 2 shows the test setup. Primary air for the combustor was driven by a Roots blower with an average velocity of 12.5 m/s slightly upstream of the dump plane. The boundary layers upstream of separation had a thickness of approximately 0.1 H, where H is the upsteam channel height, and a peak rms streamwise turbulence level between 8–10% of the mean velocity; details of the inlet profile distributions can be found in [11]. The primary air passes through a prevaporizor system where the air is preheated by two Chromalox air heaters to approximately 100°C. The preheated air then passes into an evaporation chamber where liquid JP10 is introduced using a spray nozzle. Fuel flow rates are metered via a venturi before entering the evaporator. The flow from the prevaporizor is ducted to the test facility where ignition occurs using a spark rod. A liquid ring vacuum pump is used to pull the secondary flow from the combustor by creating low pressure behind the suction gap. The high-temperature secondary flow leaving the combustor is cooled using heat exchangers before entering the liquid ring vacuum pump to avoid flashing within the pump. A venturi is placed in the secondary flow line for metering and the mass flow rate

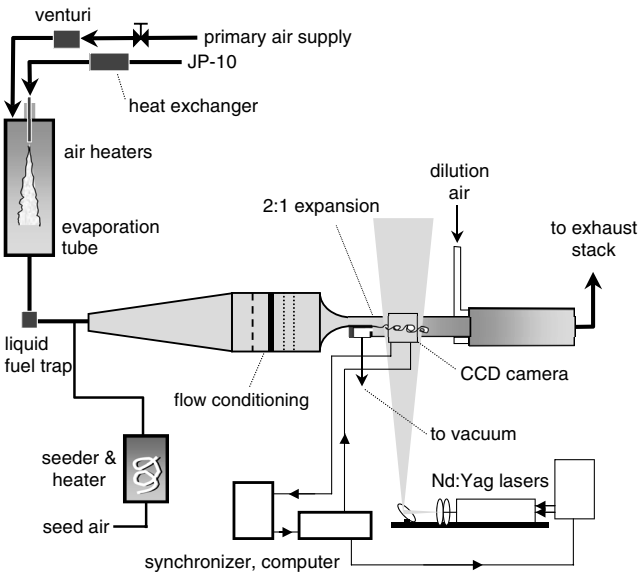

Fig. 2 Experimental setup and diagnostic configuration.

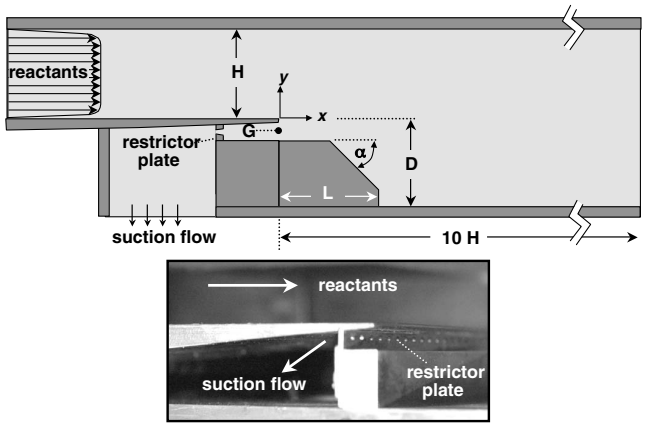

Fig. 3 Combustor geometry illustrating key parameters used to implement counterflow control.

is controlled via valves at the inlet to the pump. The water/gas discharge mixture from the vacuum pump is separated in a tank, before the gas is ducted to the exhaust stack. The discharge water is cooled via heat exchangers and then fed back in a closed loop to the vacuum pump. Dilution air is supplied to the exhaust stack to cool and dilute the combustor exhaust to prevent any unburned reactants from igniting in the stack.

Particle image velocimetry (PIV) is the primary diagnostic for the cold-flow experiments discussed next. When employing PIV, a Laskin nozzle is used to produce fine olive oil droplets that are combined with the primary air upstream of the flow conditioning plenum. Side and lower walls of the test section are fabricated from quartz allowing for optical access for the PIV diagnostic; the side-viewing window through which chemiluminescence images were captured covered a streamwise extent of x/D from 0 to 7.5. The PIV system consists of a pair of Continuum Surelite II double-pulse lasers controlled by a TSI model 610032 synchronizer. A TSI model 630046 camera [1 Mpixel charge-coupled device (CCD)] is used to take image pairs allowing for cross-correlation mode PIV. The system is controlled using a personal computer through TSI Insight software version 2.0. Each test case includes the collection of 500 vector fields, a sufficient quantity that showed good convergence of mean and fluctuating velocity statistics [16].

A schematic and photograph of the combustor test section is shown in Fig. 3. The primary flow enters the combustor via a channel of height H and span 8 H. The single-sided expansion ratio is 2:1. A step extension of length L and corner chamfering at an angle α are important parameters which will be examined. The lower image of Fig. 3 is a photograph of the step illustrating the geometric detail in this region; the parameters L and α are both equal to zero, a configuration referred to as the "baseline" combustor for the remainder of the paper. The gap height $G = 0.25$ H and the splitter plate has a carefully machined trailing-edge thickness of 0.05 H.

An ignition source, for the reacting flow experiments, is created by positioning a high-voltage arc in the low-speed zone behind the rearward-facing step. Flames established in the baseline geometry are stable and self-sustaining for lean conditions and the igniter is turned off after ignition. A continuous ignition source is needed for parametric studies when changes in the geometry (variations in L and α) create unstable flame anchors. The photograph in Fig. 3 shows the secondary flow being ducted through small nozzles in a restrictor plate, located below the trailing edge. The nozzles are used during the reacting flow experiments to inhibit possible flow reversal at the step due to the relatively high pressure fluctuations that can be experienced from unsteady heat release, particularly at equivalence ratios higher than those studied here.

Reacting Flow in Baseline Geometry

Equivalence ratios ranging from the lean stable combustion limit to slightly rich have been tested. The JP10 fuel has a low vapor pressure, which requires preheating of the air to obtain the desired

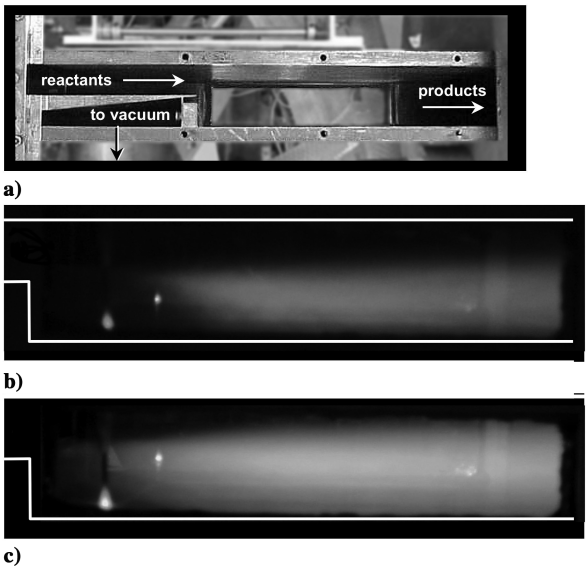

Fig. 4 Time-averaged images of the chemiluminescence of the flame with and without control: a) side view of combustion chamber, b) without counterflow control, and c) with 6% secondary mass flow.

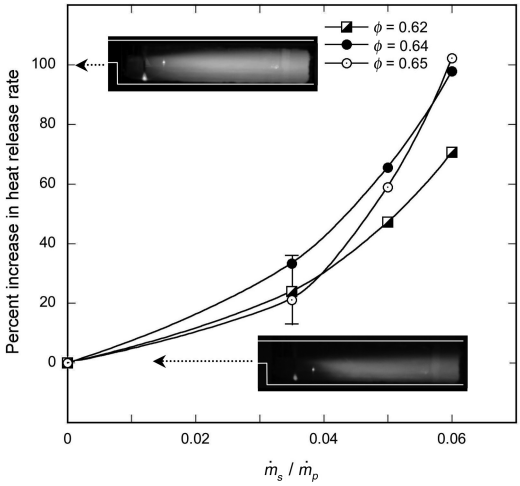

Fig. 5 Heat release rates relative to the baseline combustor obtained using filtered chemiluminescence capturing the C_2^* radical.

equivalence ratios. For rich conditions, the prevaporized fuel can condense on the combustor walls before ignition due to lower local temperatures, hence practically limiting operation to only slightly rich conditions. One of the primary advantages of operating in a premixed/prevaporized mode is the allowance for control of the thermal NO_x production through operating under sufficiently lean conditions, hence the restriction to lean toward slightly rich was deemed acceptable.

Initial combustion studies were focused on understanding affects of countercurrent shear in the self-sustained stable combustion regime, occurring for equivalence ratios up to approximately $\phi = 0.65$, i.e., for equivalence ratios where strong thermoacoustic instabilities were not present. Time-averaged images of the chemiluminescence of the flame with and without control are shown in Fig. 4 for $\phi = 0.65$, corresponding to a fuel input rate of 64 kW; a side view of the combustion chamber is also provided with the side wall removed (Fig. 4a). In the baseline configuration shown in Fig. 4b, the uncontrolled flame appears a faint blue (in the laboratory) and fills a relatively modest fraction of the expansion downstream of the step. The bright spots in the photographs slightly downstream of the dump plane and near the lower wall are the igniter rod and its reflection in the rear window. The igniter rod is turned off, but is glowing due to high temperature combustion products in the recirculation zone. Figure 4c is the averaged unfiltered chemiluminescence image as seen for $\dot{m}_s/\dot{m}_p = 0.06$, where the primary and secondary mass flow rates are indicated by subscripts p and s, respectively. Although reactant can still be observed to leave the downstream extent of the viewing window, the flame is considerably more luminous and encompasses a much greater fraction of the combustor, indicating increased volumetric heat release rates using counterflow.

In an effort to quantify the role of counterflow, an experimental technique was implemented to measure filtered flame chemiluminescence. This approach was used to obtain relative measures of changes in heat release rates with counterflow control. Chemiluminescence emission has previously been studied for premixed hydrocarbon flames by Lee and Santavicca [19] and Ikeda et al. [20]. Their studies indicate that OH^*, CH^*, CO_2^*, and C_2^* provide the primary contribution to chemiluminescence emission. Filtered flame radiation corresponding to combustion radicals such as CH^* and C_2^*, for a fixed equivalence ratio, has been shown to have a linear relationship with heat release by McManus [10] and Poinsot et al. [21]. It should be noted that this relationship has not been formally established for JP10–air mixtures, and hence should be considered a first attempt at quantifying the impact of the control on combustion efficiency. The C_2^* combustion radical has been shown to be a good indicator of heat release rates for flowfields with higher turbulence [21], and therefore was the observed radical for these experiments. The combustor was shrouded between the camera and the quartz viewing window to capture only flame radiation. The radiation was filtered at 516 nm and viewed with a 28 mm camera lens before passing into a Dantec photomultiplier tube; measurements were integrated over 30 s. The photomultiplier tube was powered by a Pacific Photometric model 204 negative high-voltage power supply; the signal was amplified with a Stanford model SR560 low-noise preamplifier and collected with an IOtech ADC488/8SA data acquisition board. Relative global heat release rate measurements were made for equivalence ratios between 0.62 and 0.65 with secondary suction mass flow rates of up to 6% of the primary mass flow.

Figure 5 shows the increase in heat release rates with counterflow control; corresponding mean flame images, at $\phi = 0.65$, are provided as insets to the figure. Heat release rates were normalized by the rates obtained for 0% counterflow. Volumetric heat release is shown to increase monotonically with counterflow control, nearly doubling with 6% suction mass pulled from the combustor at $\phi = 0.64$ and 0.65. Implementation of counterflow control was found to have the same affect on relative heat release rates, independent of equivalence ratio; no specific trends with equivalence ratio could be discerned above the uncertainty in the measurements.

The observations shown thus far are consistent with velocity field data obtained in nonreacting flow studies [11] and indicate that counterflow is effective at increasing burning in a compact environment. Although these benefits are clearly advantageous for high-speed applications where residence time is very limited, the compactness also suggests reduced timescales for mixing and ignition, which can be problematic for flame anchoring. Furthermore, isothermal studies clearly indicate that the implementation of suction at the dump plane does not provide efficient control of the shear layer separating from the step, largely because the sinklike nature of the vacuum control extracts mass principally from the low-momentum fluid residing near the lower wall of the combustor [11]. The parametric studies taken up in the next section address geometric changes that can be made to more effectively employ counterflow for combustion control above the baseline trends seen in Fig. 5.

Parametric Effects

The performance of a control mechanism is not only evaluated by its benefits but also by the penalties associated with its implementation. Although the affect of counterflow control on flame compactness and burning intensities are significant, as seen in Fig. 5, the drag associated with a 6% reverse suction flow may be too

high a penalty to justify its implementation. In an effort to achieve control at a smaller system penalty, the physics of the countercurrent shear flow in the near-field region, was considered in more detail. All parametric effects discussed next were conducted at an equivalence ratio of $\phi = 0.62$; the primary flow inlet velocity was held fixed at 12.5 m/s, providing a Reynolds number based on step height D of 1.2×10^4.

In the absence of control, the primary flow creates a recirculation zone, which naturally contains a countercurrent shear layer upstream of attachment. In isothermal studies, it was found that the role of suction in the step geometry is to draw the low-momentum fluid near the lower wall into the slot below the trailing edge [11]. The changes in the mean velocity field caused by suction are principally to increase the reverse velocity near the lower combustor wall and reduce the streamwise extent of the recirculation zone. However, while turbulent levels are increased using counterflow control, the secondary flow drawn out of the combustor does not effectively interact with the high-momentum fluid passing over the step. It is this latter effect, namely increasing countercurrent shear but also increasing the vorticity of the separating shear layer, which motivated the geometric changes studied next.

In previous work in unconfined countercurrent shear flows [13], a control surface was added to direct the secondary flow in closer proximity to the primary flow creating a shear layer with higher mean shear. The first parametric choice was to extend the backward-facing step and effectively create this control surface. In the new geometry L was increased to length D (see Fig. 3) to provide an extended surface for establishing counterflow. Alpha was kept equal to zero to maintain the bluff edge conducive for flame anchoring. This parametric configuration ($L = D$, $\alpha = 0$) is referred to as the extended step geometry for the subsequent discussion.

Figure 6 shows unfiltered exposures of the flame brush for the extended step geometry, with and without control, in the near vicinity of the trailing edge. The combustor is operating at $\phi = 0.62$. The extension of the rearward-facing step to length L has the affect of creating multiple steps within the combustor. Figure 6a shows the flame without control implementation. The flame appears faint in the near region of the step, becoming more intense downstream of the igniter; the region further downstream is quite consistent with the baseline combustor shown in Fig. 4b. The arrow in the lower image shows where secondary mass flow exits the combustor with a magnitude of 1.8% of the primary mass flow. Increased wrinkling along the flame interface can be seen in Fig. 6b, along with a strong increase in flame luminosity. The reaction zone is also seen to move upstream to the immediate vicinity of the step with the flame at times moving up into the shear layer above the step.

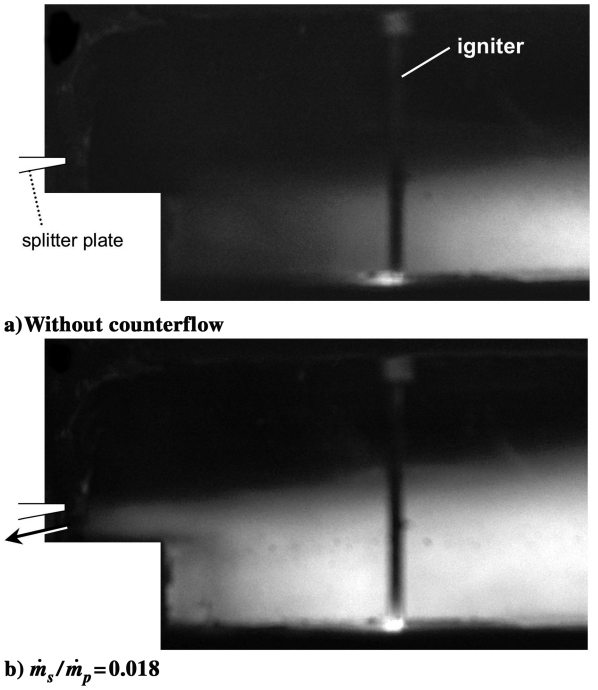

Fig. 6 Time exposures (1/10 s) of the flame in the immediate neighborhood of the trailing edge.

Although the intensity and volume of the flame appear to have increased significantly with low levels of secondary flow, the extended step geometry did not provide a suitable flame anchor. Therefore, the igniter was run continuously to sustain burning. The multistep configuration appeared to create two disconnected zones in which the flame could reside, in the countercurrent shear layer above the step and in the recirculation zone behind the extended step. Self-sustained burning requires a steady stream of hot products to come into direct contact with incoming reactants to maintain an ignition source. The shear layer above the step does not provide enough residence time for products to ignite the incoming flow and the unsteadiness of the region makes it a poor flame anchor. Even though the residence time behind the step is much larger, the products appear to be unable to reach the fresh supply of incoming reactants to maintain self-sustained ignition. Although the extended step geometry did not provide a stable mechanism for reignition and flame anchoring, the flame luminosity was significantly increased using very modest levels of secondary mass compared with the baseline configuration.

Unfiltered chemiluminescence was used to obtain more quantitative values of the observed increases in burning. Although absolute values of heat release rate are unobtainable with this diagnostic, the interest lies in finding trends in the relative heat release rates. For typical hydrocarbon flames, OH^*, CH^*, and C_2^* emission occurs over narrow wavelength bands and contributes a small portion of the overall chemiluminescence. According to Lee and Santavicca [19], CO_2^* emission contributes the majority of flame chemiluminescence and is an indication of overall heat release. The formation of soot, which causes black-body radiation, prevents the establishment of a linear relationship between flame chemiluminescence and heat release. The JP10–air mixture showed no signs of black-body radiation, therefore the unfiltered chemiluminescence is not skewed by this effect. The unfiltered chemiluminescence measurements are believed to represent emission from almost exclusively CO_2^* emission. The unfiltered chemiluminescence images were captured with a high-speed video camera through the quartz window, capturing up to nine step heights downstream of the trailing edge. The igniter was windowed out during image processing to eliminate fluctuations in luminosity. (Note that for the modified geometries, the continuous ignition source led to saturation of the photomultiplier tube, and hence a different approach was used for quantifying heat release rates.)

Figure 7 shows the effect of counterflow control on volumetric heat release rates for the extended step geometry. The data were

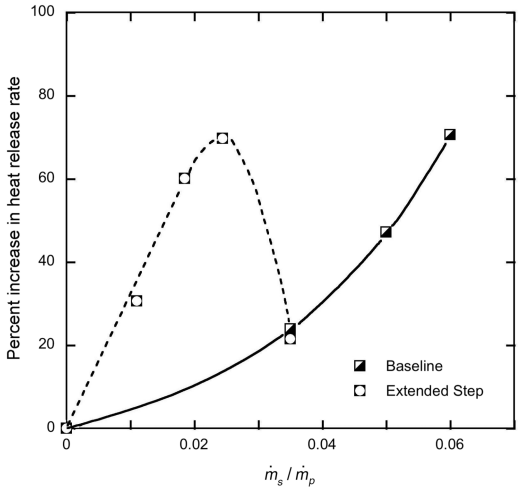

Fig. 7 Unfiltered chemiluminescence measurements for backward-facing step with extension length having L/D.

normalized by the unfiltered luminosity of the case without control. For low levels of counterflow control, the heat release rates are significantly increased as compared with the baseline geometry. For a counterflow level of $\dot{m}_s/\dot{m}_p = 0.025$, Fig. 7 shows the heat release rate to be increased by 70%, whereas the baseline geometry indicated a 15% increase for the same level of secondary flow. This suggests a substantial increase in heat release rates was obtained from adding a guiding surface for the secondary suction flow. However, as secondary flow is increased to higher levels, it begins to have a detrimental impact on combustion efficiency. From 2.5% to 3.5% counterflow levels, the heat release drops off dramatically. The luminosity of the flame is observed to decrease as well, and ignition and burning become increasingly difficult to maintain.

To gain a deeper physical understanding of the flowfield created by the extended step, and attempt to identify the source of the nonmonotonic behavior displayed in Fig. 7, the facility was reconfigured to study the extended step geometry under nonreacting (isothermal) conditions. Figure 8 shows flow conditions in the near region of the extended step and trailing edge for secondary flows between 0 and 5.2% of the primary mass using PIV. The contours show turbulence levels, calculated as the average of the rms of the streamwise and cross-stream components normalized by the average inlet velocity. The corresponding streamlines provide insight into the mean flow behavior. The baseline case without control, as seen in Fig. 8a, shows a nearly stagnant flow directly above the step, at y/D between 0 and roughly -0.2. Figure 8a also shows increasing levels of turbulence occurring in the shear layer between the primary inlet flow and the recirculation flow beginning at an x/D of 1.25. At a level of 2.4% counterflow, seen in Fig. 8b, the outermost streamlines of the large recirculation zone downstream of the step are exiting the combustor via the secondary flow route. A secondary smaller recirculation zone has now fully formed above the extended step. For a secondary suction mass flow level of 2.4%, at an x/D of 1.0, the turbulence levels have already reached 20% of the primary stream velocity, whereas in the uncontrolled case this occurs at an x/D of 1.5, providing an indication of the compactness made possible with control. As suction was increased to 3.6%, the primary flow contours show the highest turbulence levels moved upstream approximately one step height as compared with the uncontrolled case. The streamlines in Fig. 8c, however, show nearly half of the suction mass is drawn directly from the primary inlet flow, thereby not interacting with the main recirculation zone behind the main step. At the highest level of control, shown in Fig. 8d, the suction mass flow is drawn entirely from the primary flow; impingement of the primary flow can be seen on the upper surface of the step at an x/D of roughly 0.75.

Flow impingement shuts off the countercurrent shear and associated turbulence production, causing the flow to become relatively undisturbed in the shear layer over the recirculation zone. The flow blockage completely turns off the control mechanism by inhibiting secondary flow from being pulled from the main recirculation zone behind the step. It appears that the impingement point creates a low-speed buffer zone between the upper high-speed primary flow and the recirculation flow, inhibiting the production of turbulence. The sharp drop in turbulence levels downstream of the step, shown in Fig. 8d, may explain the drop in heat release rates encountered with higher levels of counterflow control for reacting conditions, as seen in Fig. 7. The drop in heat release rates could be due to a decrease in flame wrinkling caused by the sharp decline in turbulence production once the primary flow impinges on the upper wall of the step.

Based on the findings of the isothermal flow studies, a new geometry was designed to exploit the reduced secondary flow requirements, while avoiding the onset of primary flow reversal and impingement on the step. Referring to Fig. 3, the new design continued to have a step extension of $L = D$, with the modification occurring to the angle $\alpha = 45$ deg. This chamfering effect was chosen in an attempt to insure the primary flow could safely pass the step without hitting the surface. (The location of the chamfer was somewhat arbitrary, terminating at a distance of 0.35 D above the lower wall of the combustor.) The modified extended step geometry was again studied using PIV, under isothermal conditions; Fig. 9 shows the results of the experiments for two cases, with and without control. Figure 9a, shows turbulence contours of the modified extended step geometry without counterflow control and in Fig. 9b with a secondary suction mass flow rate of 5.2% of the primary mass flow. Streamlines also show the direction of the flowfield in both figures. Two streamwise PIV windows were required to capture the flowfield up to x/D of at least three. Figure 9a shows a nearly stagnant flowfield in the vicinity of x/D of 0.5 and y/D of -0.1. With control implementation of 5.2% as shown in Fig. 9b,

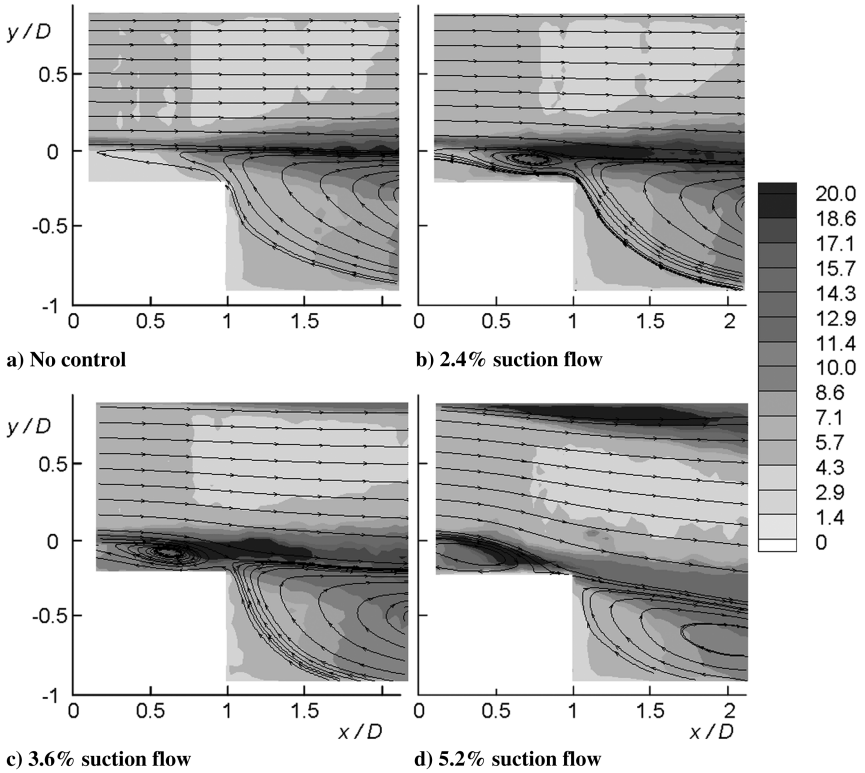

Fig. 8 Total turbulence levels and mean flow streamlines for the extended step geometry.

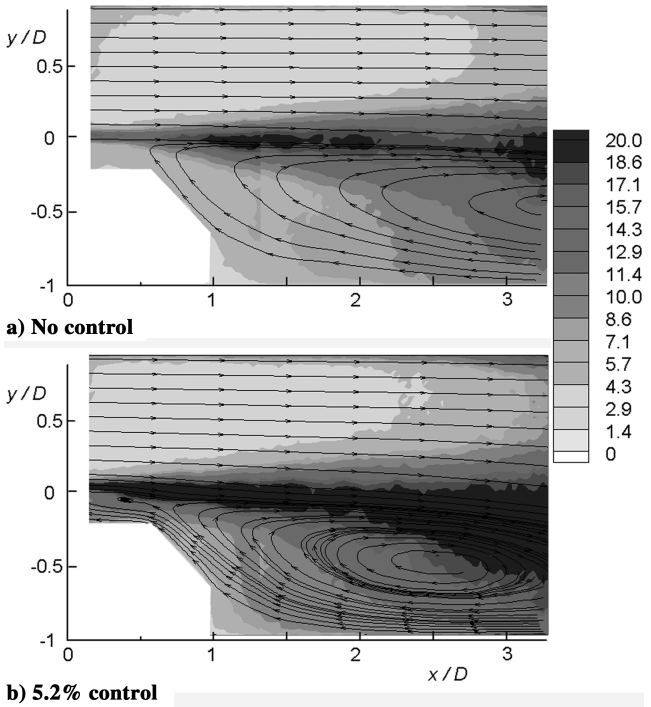

Fig. 9 Total turbulence levels and mean flow streamlines for modified step geometry.

streamlines show flow originating in the recirculation zone exiting the combustor through the restrictor plate. In Fig. 9b, directly above the step, a compact shear layer can be seen with high velocity gradients occurring over a streamwise distance comparable to the step height.

A comparison of the turbulence between Figs. 9a and 9b shows an increase in maximum levels as well as a substantial increase in the combustor volume over which the levels occurred. For the controlled case, the shear layer immediately downstream of the trailing edge at x/D equal to 0.5, is nearly twice as thick. At an x/D of 3.0, Fig. 9b shows increased turbulence levels extending over a region nearly double the uncontrolled case. The recirculation zone is also seen in Fig. 9b to be compacted, bringing the secondary flow into closer contact with the primary flow.

The isothermal experiments conducted with the modified (chamfered) step geometry indicate that the extended streamwise control in the vicinity of the trailing edge (where the shear layer begins to form) results in a reduction of the secondary mass flow required for turbulence production. At a control level of 5.2%, the modified extended step geometry (as seen in Fig. 9b) has no primary flow reversal and does not experience a secondary recirculation zone above the step, which appears to be the precursor of an attachment point on the step, as seen in Fig. 8d. The modified extended step geometry thus has increased the level of control that could be implemented without primary flow impingement on the step surface. Primary flow impingement was not encountered, up to a secondary suction level of 6%.

Based on the encouraging results of the isothermal tests, the dump combustor was once again reconfigured for burning to test the new geometry. As indicated by the PIV results, the elimination of a secondary recirculation zone with the modified extended step geometry led to a more conducive geometry for flame anchoring as compared with the extended step. However, it was not strong enough to maintain a flame for long durations of burning, therefore, the igniter was used continuously. Unfiltered chemiluminescence was used as an indicator of heat release rates. Once again, the igniter was windowed out upon image processing. Figure 10 shows the relationship of heat release rates with counterflow control in the modified extended step geometry; results for the other geometries are included for completeness.

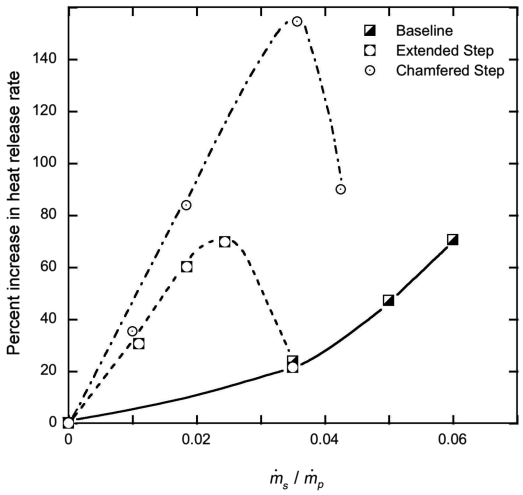

Fig. 10 Heat release rates based on unfiltered chemiluminescence.

Figure 10 indicates that the slope with counterflow control is initially much steeper than the baseline and step extension ($\alpha = 0$) geometries. At a counterflow control level of roughly 3.5% a nearly eightfold enhancement in the percent increase in heat release rate can be seen for the modified geometry as compared with the baseline geometry, thus greatly reducing the secondary mass flow requirement. The addition of a secondary surface to increase countercurrent shear flow control over a longer streamwise distance resulted in a 150% increase in relative heat release rates, thus creating compact robust combustion at lower secondary mass flow rates. At secondary mass flow rates greater than approximately 3.5% of the primary flow, the chemiluminescence results in Fig. 10 display the signature downturn as previously seen in the extended step geometry. The isothermal streamlines in Fig. 9 do not indicate the pinching-off phenomenon occurring up to 5.2% secondary flow, but care must be exercised in comparing the streamlines measured in nonreacting conditions to those anticipated with heat release. One expects the recirculation domain of the reacting flow to move upstream relative to the isothermal flowfield and therefore the pinching-off process would likely occur at lower levels of secondary flow during heat release. Although detailed measurements in the reacting flow would need to be made to verify this trend, it has been borne out in other combustors where reacting and nonreacting mean flowfields have been compared [2].

Summary

Premixed, prevaporized JP10 and air were burned in a modified dump combustor employing a fluidic control mechanism aimed at elevating turbulent kinetic energy, with the overall goal of increasing volumetric heat release rates. A secondary flow was pulled from the combustor immediately below the trailing edge via a suction pump to strengthen the countercurrent shear layer naturally created by the dump configuration. Chemiluminescence measurements were used to quantify the effect of control on heat release rates, showing a 100% increase in burning, as normalized by the uncontrolled case, with 6% suction mass flow exiting the combustor. Parametric effects were studied in an effort to reduce losses associated with control implementation. A rearward-facing step extending beyond the trailing edge was examined and showed a decrease in secondary mass flow requirements by half to achieve a comparable level of combustion enhancement. However, relative heat release rates dropped off sharply as secondary mass flow levels exceeded 2.5% of the primary mass flow. PIV measurements conducted under isothermal flow conditions for this geometry indicated the drop off in heat release rate was linked to a drop in turbulence levels due to primary flow impingement on the upper surface of the lengthened rearward-facing step. To avoid flow impingement, the bluff edge of the lengthened step was removed, resulting in increased control capability. Countercurrent shear control is shown to be a promising

control mechanism for creating compact, robust combustion in the confined dump combustor geometry. Parametric modification enabled the implementation of the control mechanism over a longer streamwise distance, resulting in a 150% increase in heat release rates at half the secondary mass flow requirement.

Acknowledgments

The authors would like to acknowledge the generous support of the Office of Naval Research under contract N00014-01-1-0644, as well as the valuable assistance we have received from D. Forliti and J. Lutz. We have also benefited considerably from the continued guidance that we have received from the Office of Naval Research technical monitor, G. D. Roy.

References

[1] Eaton, J. K., and Johnston, J. P., "Review of Research on Subsonic Turbulent-Flow Reattachment," *AIAA Journal*, Vol. 19, No. 9, 1981, pp. 1093–1100.

[2] Pitz, R. W., and Daily, J. W., "Combustion in a Turbulent Mixing Layer Formed at a Rearward-Facing Step," *AIAA Journal*, Vol. 21, No. 11, 1983, pp. 1565–1570.

[3] Gabruk, R. S., and Roe, L. A., "Velocity Characteristics of Reacting and Nonreacting Flows in a Dump Combustor," *Journal of Propulsion and Power*, Vol. 10, No. 2, 1994, pp. 148–154.

[4] Adams, E. W., and Johnston, J. P., "Effects of the Separating Shear Layer on the Reattachment Flow Structure Part 1: Pressure and Turbulence Quantities," *Experiments in Fluids*, Vol. 6, No. 6, 1988, pp. 400–408.

[5] Adams, E. W., and Johnston, J. P., "Effects of the Separating Shear Layer on the Reattachment Flow Structure Part 2: Reattachment Point and Wall Shear Stress," *Experiments in Fluids*, Vol. 6, No. 7, 1988, pp. 493–499.

[6] Driver, D. M., and Seegmiller, H. L., "Features of a Reattaching Turbulent Shear Layer in Divergent Channel Flow," *AIAA Journal*, Vol. 23, No. 2, 1985, pp. 163–171.

[7] Smith, D. A., and Zukoski, E. E., "Combustion Instability Sustained by Unsteady Vortex Combustion," *AIAA/SAE/ASME/ASEE 21st Joint Propulsion Conference, Monterey, CA*, AIAA Paper 85-1248, July 1985.

[8] Yu, K. H., Trouve, A., and Daily, J. W., "Low-Frequency Pressure Oscillations in a Model Ramjet Combustor," *Journal of Fluid Mechanics*, Vol. 232, Nov. 1991, pp. 47–72.

[9] Schadow, K. C., Gutmark, E., Parr, T. P., Parr, D. M., Wilson, K. J., and Crump, J. E., "Large-Scale Coherent Structures as Drivers of Combustion Instability," *Combustion Science and Technology*, Vol. 64, Nos. 4–6, 1989, pp. 167–186.

[10] McManus, K. R., "Effects of Controlling Vortex Formation on the Performance of a Dump Combustor," Stanford Univ., Palo Alto, CA, Topical Rept. T-262, June 1990.

[11] Forliti, D. J., and Strykowski, P. J., "Controlling Turbulence in a Rearward-Facing Step Combustor Using Countercurrent Shear," *Journal of Fluids Engineering*, Vol. 127, No. 3, 2005, pp. 438–448.

[12] Strykowski, P. J., Krothapalli, A., and Jendoubi, S., "Effect of Counterflow on the Development of Compressible Shear Layers," *Journal of Fluid Mechanics*, Vol. 308, Feb. 1996, pp. 63–96.

[13] Strykowski, P. J., and Wilcoxon, R. K., "Mixing Enhancement due to Global Oscillations in Jets with Annular Counterflow," *AIAA Journal*, Vol. 31, No. 3, 1993, pp. 564–570.

[14] Forliti, D. J., Tang, B. A., and Strykowski, P. J., "Experimental Investigation of Planar Countercurrent Turbulent Shear Layers," *Journal of Fluid Mechanics*, Vol. 530, May 2005, pp. 241–264.

[15] Strykowski, P. J., and Niccum, D. L., "Stability of Countercurrent Mixing Layers in Circular Jets," *Journal of Fluid Mechanics*, Vol. 227, June 1991, pp. 309–343.

[16] Strykowski, P. J., and Niccum, D. L., "Influence of Velocity and Density Ratio on the Dynamics of Spatially Developing Mixing Layers," *Physics of Fluids A*, Vol. 4, No. 4, 1992, pp. 770–781.

[17] Huerre, P., and Monkewitz, P. A., "Absolute and Convective Instabilities in Free Shear Layers," *Journal of Fluid Mechanics*, Vol. 159, Oct. 1985, pp. 151–168.

[18] Monkewitz, P. A., and Huerre, P., "Influence of the Velocity Ratio on the Spatial Instability of Mixing Layers," *Physics of Fluids*, Vol. 25, No. 7, 1982, pp. 1137–1143.

[19] Lee, J. G., and Santavicca, D. A., "Experimental Diagnostics for the Study of Combustion Instabilities in Lean Premixed Combustors," *Journal of Propulsion and Power*, Vol. 19, No. 5, 2003, pp. 735–750.

[20] Ikeda, Y., Kojima, J., and Nakajima, T., "Local Chemiluminescence Measurements of OH^*, CH^*, and C_2^* at Turbulent Premixed Flame Fronts," *Smart Control of Turbulent Combustion*, edited by A. Yoshida, Springer–Verlag, Tokyo, 2001, pp. 12–27.

[21] Poinsot, T. J., Trouve, A. C., Veynante, D. P., Candel, S. M., and Esposito, E., "Vortex Driven Acoustically Coupled Combustion Instability," *Journal of Fluid Mechanics*, Vol. 177, April 1987, pp. 265–292.

J. Gore
Associate Editor